The Iraqi Journal For Mechanical And Material Engineering, Vol.18, No2, June 2018

MICROSTRUCTUR AND MICROHARDNESS OF LASER CLADDING Ni BASED ON COLD ROLLED STEEL

Maryam Abduladhem Ali Bash Ali Munther Mustfa Ali Mezher Resan
Firas Farhan Sayyid Adnan Ibraheem Mohammed
Department of Production Engineering and Metallurgy
University of Technology, Baghdad, Iraq
Maryam_uot@yahoo.com

ABSTRACT

A study is reported of the laser cladding of a nominal composition of Ni 5 wt% Al on cold rolled low carbon steel (0.16 wt% C), using a high power continuous CO_2 laser. The severe rolled microstructure of steel was changed considerably at the heat affected zones under all specific energies. The cladded coatings showed the presence of ɣ solid solution and β (NiAlFe) phases. Sound metallurgical bonding with absence of porosity and cracks was observed between the substrate and the clad coat at specific energy higher than 80 J/mm2. The ferrite and pearlite microstructure of the substrate was changed to martensite at the region adjacent to the clad interface. It followed by large grains of austenite/ferrite and pearlite (grain growth zone), fine grains of austenite/ferrite and pearlite (recrystallization zone) and very small zone of relatively small change of cold structure (recovery zone). The last zone was confirmed by micro hardness as a recovery zone.

This investigation confirms clearly the possibility of formation different structures of grain growth, recrystallization and recovery at the laser heat affected cold rolled low carbon steel. The observed results suggest the developing of a new technique to obtain tentative functionally graded material.

KEYWORDS : Cold rolled steel; High power laser; Functionally graded material; Recrystallization; Grain growth; Recovery

البنية المجهرية والصلادة الدقيقة للاكساء بالليزر لاساس نيكل على الصلب ألمدرفل على البارد

مريم عبد االعظيم باقر علي باش علي مزهر رسن علي منذر مصطفى
فراس فرحان سيد عدنان ابراهيم محمد
الجامعة التكنولوجية / قسم الانتاج والمعادن

الخلاصة

تضمن البحث دراسة الاكساء بالليزر نو القدرة العالية نوع ثاني اوكسيد الكربون للصلب الكربوني المدرفل على البارد والحاوي على 0.16 wt% كربون باستخدام مزيج من مسحوق النيكل الحاوي على 5 wt% المنيوم. تغييرت البنية المجهرية المدرفلة بشدة للصلب بصورة مستمرة في المنطقة المتأثرة بالحرارة عند كل قيم الطاقة النوعية المستخدمة. اوضحت طبقات الاكساء الناتجة وجود طور المحلول الجامد كاما و بيتا (المركب الوسطي من النيكل والألمنيوم والحديد). تم الحصول على ربط ميتالورجي خالي من العيوب عند الحد الفاصل بين طبقات الاكساء وسطح الصلب عند قيم طاقة نوعية اكبر من 80 جول/ملم^2. تحولت البنية المجهرية للفرايت والبيرلايت في الصلب الى المارتنزايت عند الحد الفاصل للاكساء. بعدها تكونت البنية المجهرية من حبيبات من الاوستنايت / الفرايت والبيرلايت ذات حجم كبير (منطقة النمو البلوري) وبعدها حبيبات ناعمة من الاوستنايت ولفرايت والبيرلايت (منطقة اعادة التبلور) واخيرا منطقة صغيرة جدا ذات بنية مجهرية تختلف قليلا عن البنية المجهرية للصلب المشكل (منطقة الاستعادة). أوضحت النتائج الحصول على تطوير تقنية جديدة لتكوين مواد متدرجة وظيفيا كاذبة .

Received: 2017 - 5 - 31
Accepted: 2017 - 9 - 12

INTRODUCTION

The Ni-Al alloys contain high amount of Ni have been considered for long time as important alloys having high mechanical properties to be used at high temperatures Darolia et al. (1996). The Ni rich alloys with Al is consisting of high volume fraction of intermetallic compound B2 phase of NiAl (β) with L12 ordered phase of ɣ' (Ni3Al) in the matrix of Ni-solid solution (ɣ) Chenf et al. (1998). On the other hand, the rapid solidification melting or coatings techniques may play an important role to enhance further the properties of Ni-Al alloys Wei et al. (1993), Zhang et al. 2011). The rapid solidification of Ni-Al alloys could be achieved by laser cladding to produce rapid (solidification deposits on many cheap substrates such as plan carbon steels Dutta Majumdar and Manna (2011), Toyserkani et al. (2005). Many advanced technologies are getting great benefit from laser surface engineering. Among of these is laser cladding which have high flexibility to deposit many alloys. It has many advantages compared with many surface coating techniques Jayakumar et al. (2015), Torims (2013), Birger et al. (2011). It characterizes with small control dilution region, rapid solidification, clean surface and narrow heat affected zone Komvopoulos and Nagarathnam (1990), Tibblin (2015). Laser cladding using continuous feeding of a powder into the laser melt pool has the most powerful coating technique to deposit many different alloys on substrates. These cladding are capable for melting control depth of substrate and the feeding powder. The clad coatings have excellent properties of homogenous chemical composition, novel microstructure, sound interface, high hardness, excellent wear and corrosion resistance Zhong and Liu (2010), Soodi (2013), Xu et al. (2017). These features of clads may have extra combined improvement of the substrate due to the phase transformation associated with heat transfers from the fusion of clad region down to the substrate Barekat et al. (2016), Mahmoud and El-Labban (2014). The most important structural alloys widely used for many applications which require medium mechanical properties and chemical stability are low carbon steels Lin et al. (2013). These materials may consider as important cheap substrates for deposition clad coatings for many high corrosion and oxidation resistance alloys such as Ni-Al alloys Li et al. (2006). At the same time to modify the microstructure of cold rolled low carbon steel to maintain high ductility with medium strength, the acceptable and applicable strengthening mechanism is the grain refining by recrystallization Kanga et al. (2010). Generally, laser heating or melting of steels could increase the hardness due to the local phase transformation Dutta Majaumdar and Manna (2003), Kempena et al. (2011), Lee et al. (2009). This is only correct for normalized microstructure. Presence of severe deformed microstructure may produce complex responses. It appears that the laser cladding of cold rolled low carbon steel with Ni-Al alloy can enhance two important properties. These are wear and corrosion resistance from the clad deposit and high ductility and strength from the heat affected zone.

EXPERIMENTAL PROCEDURES

Samples of cold rolled low carbon steel with 0.16 wt% C (Fe-0.16% C, 0.6-0.9% Mn, < 0.05% S and < 0.04% P) with dimensions 5 cm x 2 cm x 0.3 cm were used as substrates for laser cladding. Laser cladding of the shot blasted substrate were carried out using a high power continuous wave CO_2 laser. The laser power (P) employed was 1.8 kW. The samples were traversed relative to the defocused 2.5 mm laser spot size (d) at different speeds (V) (1.5, 3.2, 4.8, 6.6, 9.1 and 12.5 mm/s). The corresponding specific energies (P/dV) are 480, 225, 150, 109, 79 and 58 J/mm^2. The average particle sizes of nickel and aluminum powders are 55 and 63 µm respectively. The feeding rate of the injection premixed powder of Ni- 5 w%t Al was 10 g/min. Low rate of argon gas (5 SLPM) was blown to protect the melted pool from oxidation. Table 1 listed the laser parameters and laser processing parameters employed.

The processed laser clads were examined metallographically using standard metallography procedures for optical and scanning electron microscopy. The samples were cut perpendicular to the cladding thickness using wire cutting. The cutting samples were cold mounted and then grinding with 500 and 1000 SiC grid emery papers. These ground samples were polished with 1 µm diamond paste. Two etching solutions were used, 3% Nital to resolve the microstructure of heat affected zones and substrate and a mixture of 50% cm^3 HCl and 50% cm^3 HNO_3 for clad regions. The microhardness of the transverse clad region and different regions of heat affected zones and substrate were measured from Vickers microhardness test using 300 g load. The microhardness of the different zones was measured by determining the corresponding microstructure from the microscopy equipped with microhardness tester.

The chemical compositions of the clad regions were measured using energy dispersive spectroscopy (EDS) equipped with scanning electron microscopy. More detail regarding the experiment work can be found elsewhere Maryam et al. (2017).

RESULTS AND DISCUSSION

Figure(1) shows the microstructure of the cold rolled low carbon steel at different magnifications. It is clearly reveals the heavily deformed grains of perlite and ferrite in the direction of the deformed occur. Higher magnification of the microstructure shows the blocks of the phases which highly raise the texture effect. This microstructure with dependent direction mechanical properties has a detrimental effect. Therefore, it is very necessary to overcome this disadvantage by heat treatment. Figure(2) shows the typical low magnification of cladded samples in which the laser performs the formation of clad due to interaction between the incident laser beam with the powder. Melting of the powder as well as part of the substrate was occurred immediately at a time dependent on the traverse speed and laser beam diameter ($t = d/v$). Then the melt pool was advanced further through the substrate where the solidification taken place by rapid heat conduction from the substrate. These conductions of solidification produce metallurgical bonding without any defects of porosity and cracks as can be shown in figures (3 and 4). As a result of increasing the specific energy the melting of the substrate and the dilution were increased. Higher specific energy has two adverse typical effects; firstly, increasing the thickness of the clad coating (Table 2) and area of heat affected zone (Figure 5). Secondly, the chemical composition of clad region changes continuously from the chemical composition of the injected powder from the upper surface of clad toward the interface (Figure 6). This behavior is related directly to the dilution of the clad region from the steel substrate. There are wide spectrum of thickness and composition of the clad coatings at different specific energies. In general, the minimum dilution with a sharp metallurgically bonded interface should be obtained to avoid the change in chemical composition from the starting powder. The interesting features were observed from the adjacent phase transformation and heat affected zones below the bonding interface. These features are totally different than those obtained from laser cladding on hot rolled substrates Ellis et al. (1995). Figure (6) shows higher magnification of the typical microstructural changes of the deformed microstructure of the substrate to produce different microstructure associated with the heating the substrate. Figures(2 and 6) postulate clearly the duplex mechanisms of martensitic phase transformation and recrystallization. There are four zones formed below the bonding interface namely (i) martensitic phase transformation, (ii) grain growth, (iii) recrystallization and (iv) recovery. The formation of martensitic zone (Figures 6d and e) is due to rapid cooling from the austenitic formation range. The temperature is believed to be higher than 1000 ^oC (according to the Fe-C phase diagram). The presence of some grains of austenite (not ferrite) is due to the lower diffusion time which is not sufficient to produce homogenous super saturated of carbon in austenite (Figure 6c). This was confirmed from microstructure due to the absence of equiaxed and interconnected grains associated with ferrite.

Therefore, the microstructure is consisted of small amount of austenite, ferrite and perlite. The low temperatures rises at the substrate below the martensitic zone suggest that the temperatures are less than 1000 ^{o}C and may reaching less than 300 ^{o}C near to the substrate (Figure 6b). The short interaction times which are sufficient to all these heat treatments of grain growth, recrystallization and recovery are believed to be due to the high stored internal energy in the deformed substrate. Higher temperatures below to the temperature of martensitic transformation are sufficient to produce grain growth of the deformed microstructure (Figures 6c and d) .

Microhardness measurements for all zones below the clad coatings showed values higher and lower than those of the deformed substrate. The maximum hardness was found at the martensitic phase transformation zone and the lower at the grain growth zone (Table2). The higher hardness of the heat affected zone was observed at the martensitic transformation zone while the lower hardness was found at the grain growth zone (Figuress. 3, 4 and 6 and Table 2). The lower hardness of the grain growth zone is due to complete removal of line defect (dislocation) and point defect present in the deformed structure. Careful examination of the deformed structure and the formation of austenite structure at room temperature suggest the heavy deformation and high stored energy. This is evident from the lower interaction time which is sufficient for changing the structure due to the stored energy. It should be reported that the hot rolled substrate will produce totally different heat affected zones Ellis et al. (1995) . Optical microscopy and scanning electron microscopy analysis of the transverse sections of the single clads show that the chemical composition of the clad regions depends heavily on specific energy. The chemical compositions of the clad regions are shifted from the standard mixed powder. The average amount of Ni at the clad regions is far from the standard value at the mixed powder as observed from EDS and EPMA (Figure 7). This is explained previously due to the strongly dependent on the area dilution associated with processing parameters Maryam et al. (2017). The laser surface cladding of low carbon steel lead to laser melting of part of the substrate which mixed with melted powder into the melt pool producing clads with different dilution from the substrate .

Examination of the microstructure shows the less dependent of the microstructure on laser processing parameters. This was found to be due to the phases formed which are mostly based on the Ni solid solution contains different amount of iron and aluminum (Figure 8). The phases produced are mostly Ni solid solution (ɣ)/Ni_3Al (ɣ') and intermetallic compound based on NiAlFe (β). The amount of ɣ phase observed is small compared with ɣ'. The microstructures of the clad regions are cellular structure due to the rapid cooling rates. These high cooling rates are due to the rapid solidification which generates heating to the adjacent substrate with different cooling rates dependent to the distance from the cladding interface (Figures. 2, 4 and 7) .

CONCLUSIONS

1- Thin single tracks with typically 80 to 580 μm clad thickness was produced without defects. The hardness of clads varies between 1.90 to 2.8 GPa at the outer surfaces dependent on the specific energy.

2- The microstructure of the laser cladding of Ni-5 wt% Al do not depend on the laser specific energy regardless the different percentage of dilution from the steel substrate. They consist of Ni- solid solution (ɣ)/ɣ' (Ni_3Al) and β (NiAl) phases.

3- Four different heat affected zones namely martensitic, grain growth, recrystallization and recovery were formed. The maximum hardness was found at the martensitic region near the interface between clad and heat affected zones.

4- The deformed ferrite and pearlite microstructure of cold rolled low carbon steel substrate changed to austenite/ferrite and pearlite at the center of the heat affected zone.

Table 1. Laser and processing parameters studied.

TEM laser mode	00
Raw laser beam diameter, D	20 mm
Focal length, f	125 mm
Shrouding gas, Argon	2.2 SLPM
Laser power, P	1.8 kW
Laser beam diameter, d	2.5 mm
Traverse speed, V	1.5-12.5 mm/s
Interaction time (d/V), t	0.2-1.67 s
Power density, P_A ($4P/\pi d^2$)	367 W/mm^2
Specific energy, S (P/dV)	58-480 J/mm^2

Table 2. Typical Microhardness measurements at different regions of clad and heat affected zones for different specific energies.

Specific energy / Location	480 J/mm^2	150 J/mm^2	109 J/mm^2	79 J/mm^2
Total thickness of clad region, µm	579	256	146	78
50 µm from outer surface	282	263	218	188
Centre of the clad region	266	252	212	-
50 µm from the interface	216	186	180	-
Martensitic zone	412	422	418	421
Grain growth zone	124	118	122	118
Recrystallization zone	196	201	185	193
Recovery zone	245	242	252	246
Cold rolled substrate	260	260	260	260

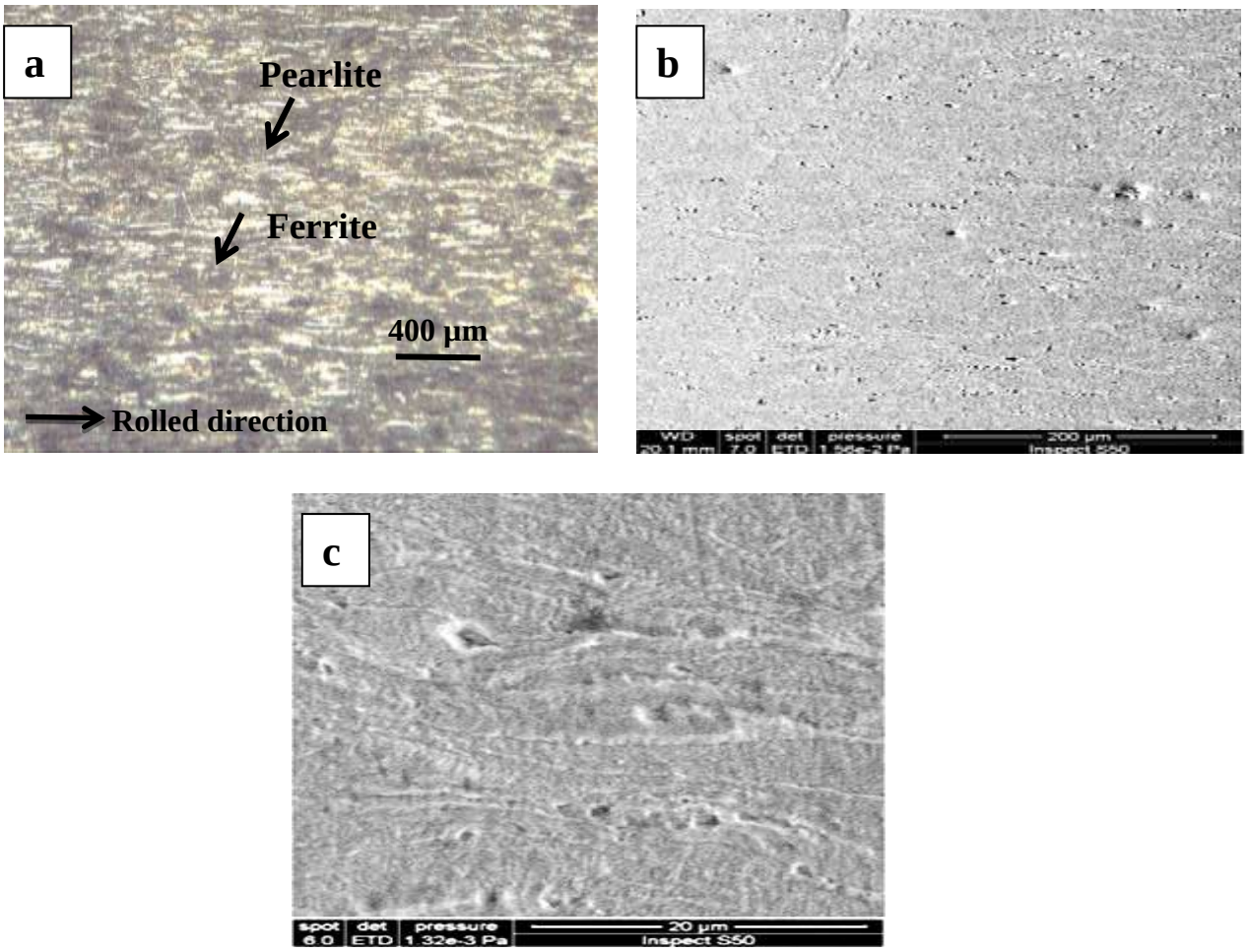

Fig.1. Microstructure of cold rolled low carbon steel (a) optical microscopy, (b) and (c) scanning electron microscopy showing the deformed ferrite and perlite at the rolling direction.

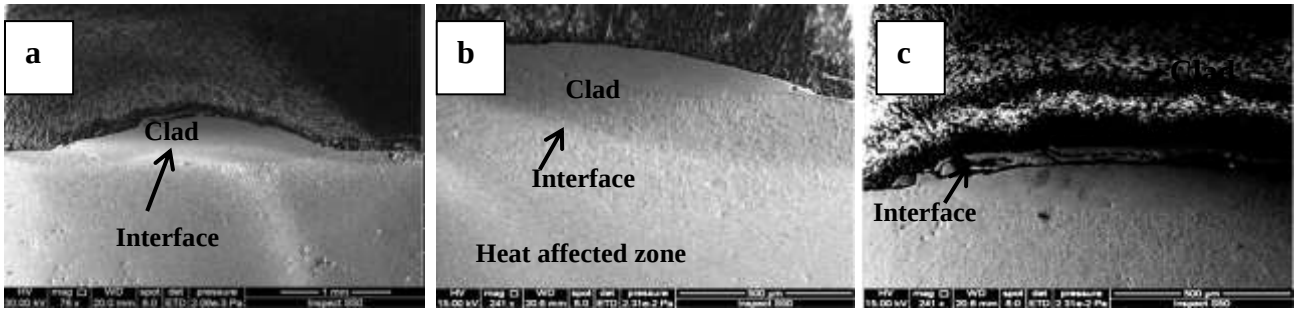

Fig. 2. Typical transverse section views of Ni-5 wt% Al clad at specific energies showing the clad regions and different zones formed at the heat affected zone (a) 220 J/mm^2, (b) 150 J/mm^2 and (c) 48 J/mm^2.

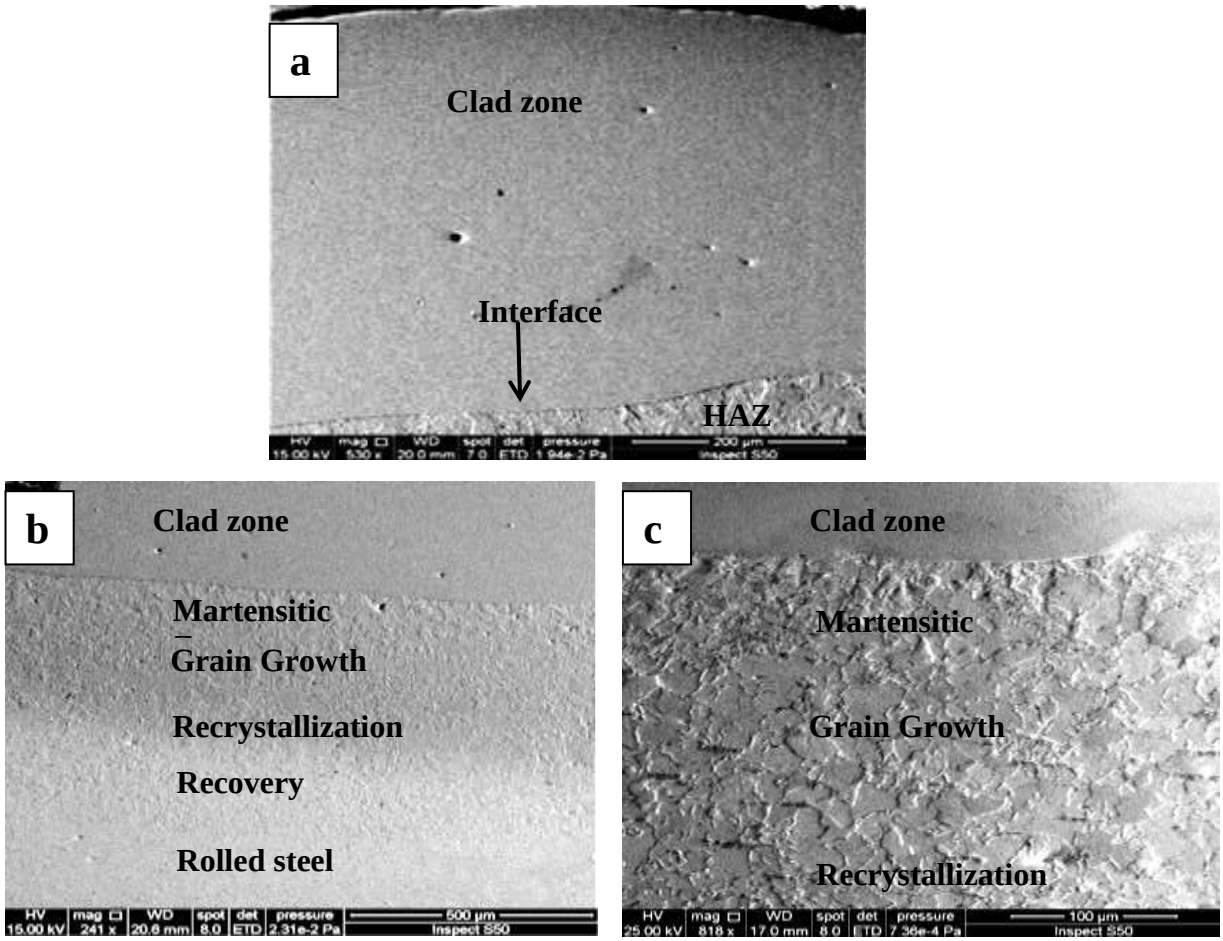

Fig. 3. Typical scanning electron micrographs of transverse section of Ni-5 wt% Al clad
(a) low magnification showing the sound clad and interface,
(b) low magnification of interface clad coating, interface, different regions of heat affected zone and substrate and
(c) higher magnification showing the martensitic structure near the interface.

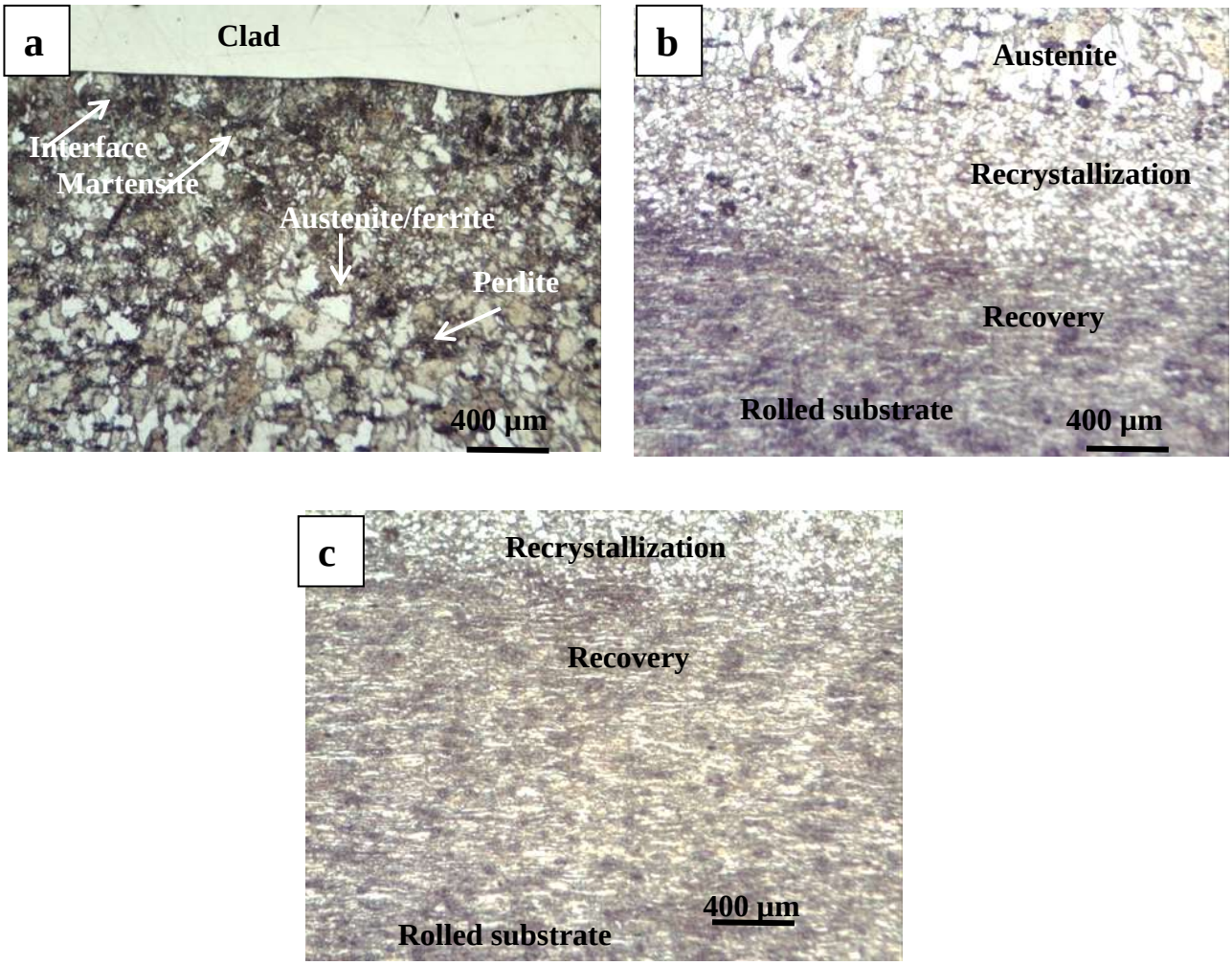

Fig. 4. Typical optical micrographs of transverse section of Ni-5 wt% Al clad
(a) low magnification showing the sound clad and interface, martensitic structure near interface and mixture of equaxied autenite and perlite,
(b) grain growth region of autenite and perlite, fine cells of austenite and perlite at recrystalization region, slightly changed of deformed structure at recovery region and rolled structure at the substre and
(c) Higher magnification showing the recrystalization and recovery zones.

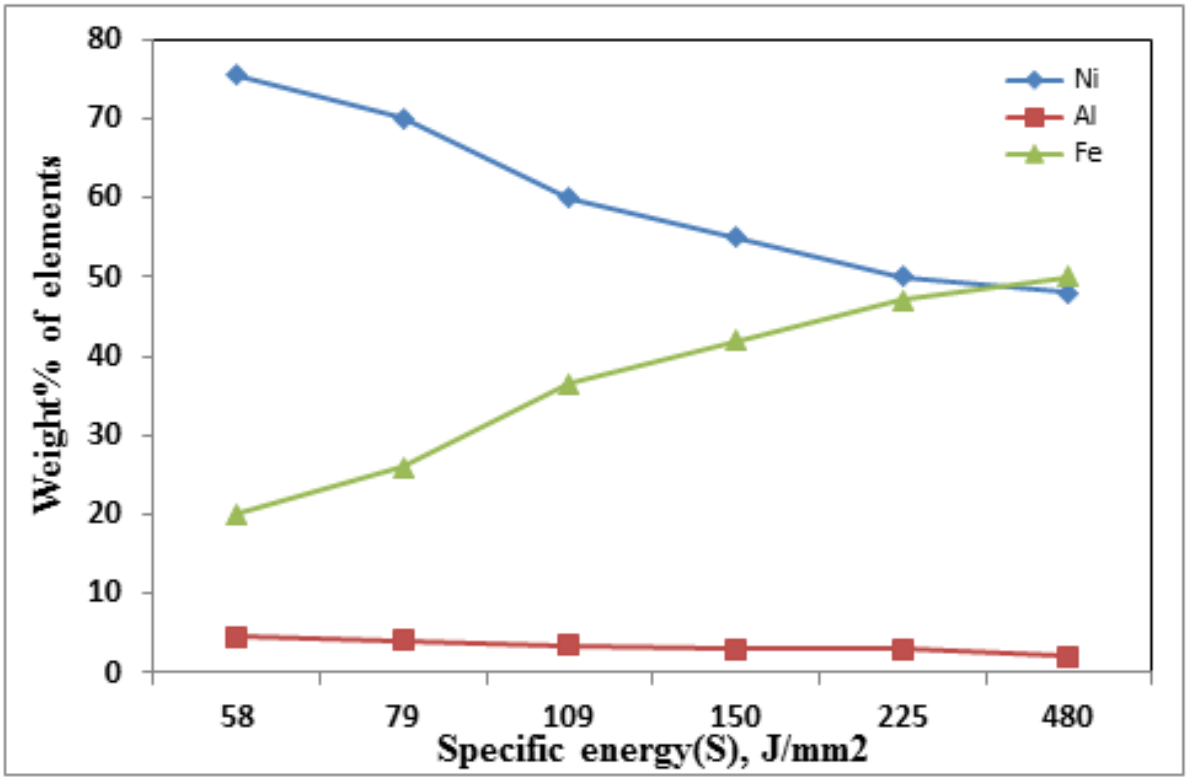

Fig. 5. The average wt% of Ni, Al and Fe in the center of clad regions processed at different specific energies.

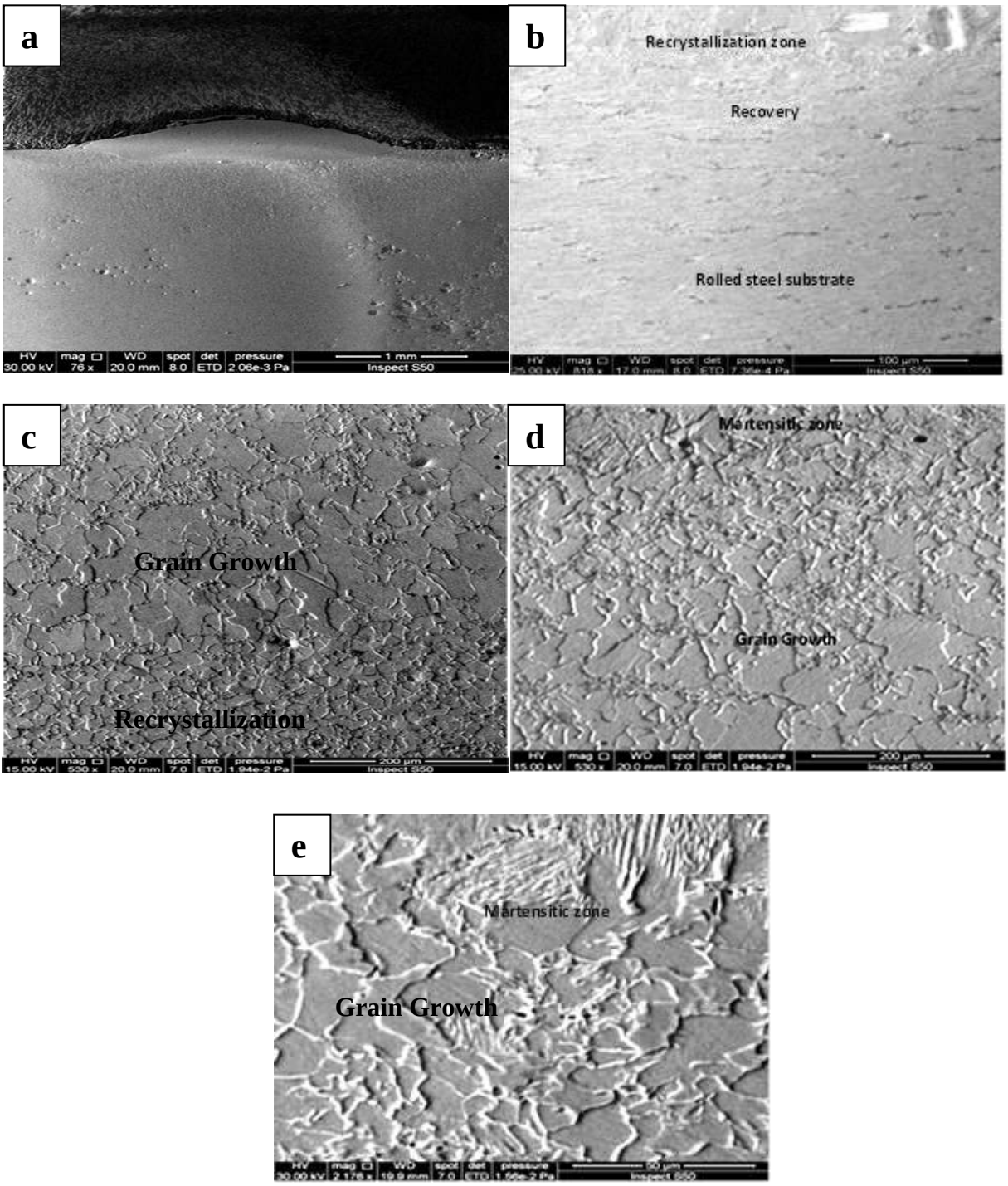

Fig. 6. Scanning electron micrographs showing the detail of clad region and heat affected zones
(a) low magnification,
(b) the functionally graded structure of recrystallization, recovery and substrate
(c) interface between grain growth and recrystallization zones
(d) zones of martensite and grain growth zones and
(e) detail of martensite and grain growth zones.

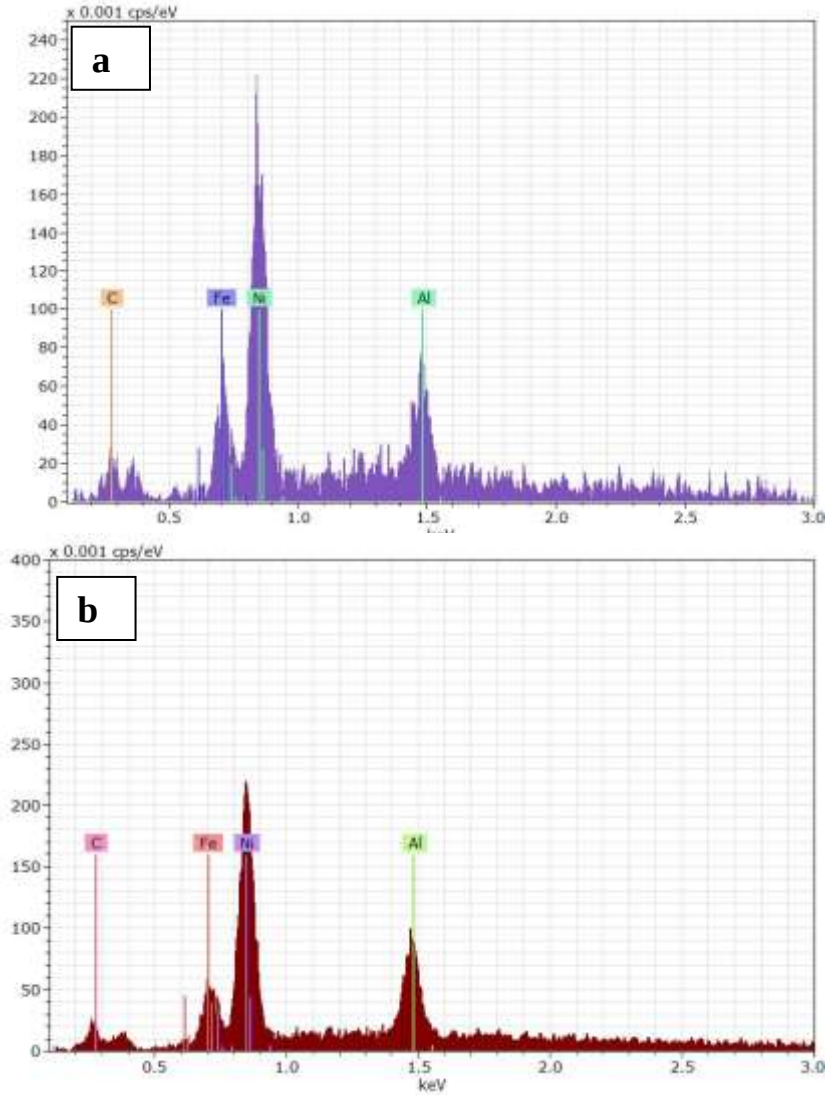

Fig. 7. EDS analysis of clad region processed at 100 J/mm^2 specific energy **(a)** near interface and **(b)** at the center of clad region.

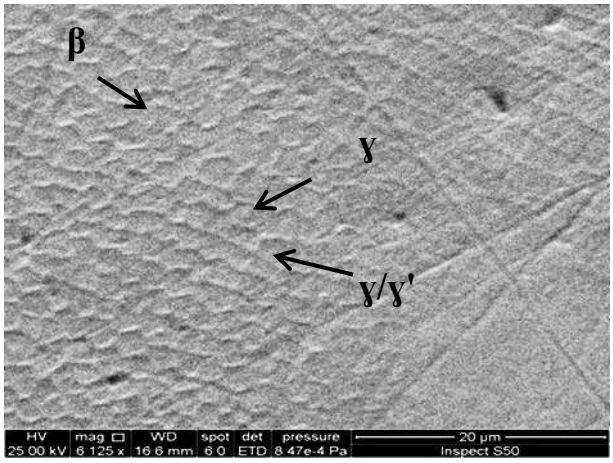

Fig. 8. Typical microstructure of clad region showing the presence of ɣ/ɣ' and β phases.

REFERENCES

Barekat M, Shojarazavi R, Ghasemi A, Nd:YAG laser cladding of Co-Cr-Mo alloy on γ-Ti Al substrate, Optics and Laser Technology, 80(2016)145-152.

Birger EM, Moskvitin GV, Polyakov AN, Arkhipov VE, Industrial laser cladding: current state and future, Welding International, 25(2011)234–243.

Cheng T, Lorser W, Leonhardt M, Effects of composition on microstructures of rapidly solidified Ni–Al alloys, J. of Materials Science, 33(1998)4365-4374.

Darolia R, Walston WS, Nathal MV, NiAl alloys for turbine airfoils, The Minerals, Metals and Materials Society, 48(1996)561-570.

Dutta Majumdar J, Manna I, Laser processing of materials, Sadhana, 28(2003)495-562.

Dutta Majumdar D, Manna I, Laser material processing, International Materials Reviews, 56(2011)341-388.

Ellis M, Xiao DC, Lee C, Steen WM, Watikns KG, W.P. Brown WP, Processing aspects of laser cladding an aluminum alloy onto steel, J. of Materials Processing Technology, 52(1995)55-67.

Jayakumar K, kumar TS, Shanmugarajan BA, Review study of laser cladding processes on Ferrous substrates, International Journal of Advanced Multidisciplinary Research 2(2015)72-87.

Kanga S, Junga Y, Junb J, Lee Y, Effects of recrystallization annealing temperature on carbide precipitation, microstructure, and mechanical properties in Fe-18Mn-0.6C-1.5Al TWIP steel, Materials Science and Engineering: A, 527(2010)745-751.

Kempena K, Yasa E, Thijs L, Kruth JP, Van Humbeeck J, Microstructure and mechanical properties of Selective Laser Melted 18Ni-300 steel, Physics Procedia 12(2011)255-263.

Komvopoulos K, Nagarathnam K, Processing and characterization of laser-cladded coating materials, Journal of Engineering Materials and Technology, 112(1990)131-143.

Lee J, Jang J, Joo B, Son Y, Moon Y, Laser surface hardening of AISI H13 tool steel, Trans. Nonferrous Metallurgical Society China,19(2009)917-920.

Li Y, Liu Y, Geng H, Nie D, Synthesis and cladding of $N_{i3}Al$ intermetallic on steel substrate by laser controlled reactive synthesis, Journal of Materials Processing Technology, 171(2006)405-410.

Lin P, Zhang Z, Zhou, Ren L, The mechanical properties of medium carbon steel processed by a biomimetic laser technique, Materials Science and Engineering: A, 560(2013)627-632.

Mahmoud ERI, El-Labban HF, Microstructure and wear behavior of TiC coating deposited on spheroidized graphite cast iron using laser surfacing, Engineering, Technology and Applied Science Research, 4(2014)696-701.

Maryam A. Ali Bash, Frais FS, Adnan IM, Ali MM, Ali MR, Effect of feed rate on laser surface cladding of cold steel, The first International Scientific Conference of Nanotechnology and Advanced Materials in the Petroleum and Gas Industry, University of Technology, Baghdad, Iraq, 2017.

Soodi M, Investigation of Laser Deposited Wear Resistant Coatings on Railway Axle Steels, MSc thesis, RMIT University, 2013.

Tibblin F, Characterization of a newly developed martensitic stainless steel powder for Laser and PTA cladding, KTH Institute of technology, Industrial engineering and management, 2015.

Torims T, The application of laser cladding to mechanical component repair, renovation and regeneration, Daaam International Scientific Book, 2013, Chapter 32, pp. 587-608.

Toyserkani E, Khajepour A, Corbin C, Laser cladding, 2005 by CRC Press LLC.

Wei B, Herlach DM, Ommer FS, W. Kurz W, Rapid solidification of undercooled eutectic and monotectic alloys, Materials Science and Engineering: A, 173(1993)355-359.

Xu X, Mi G, Chen L, Xiong L, Jiang P, Shoa X, C. Wang C, Research on microstructures and properties of Inconel 625 coatings obtained by laser cladding with wire, Journal of Alloys and Compounds, 715(2017)362-373.

Zhang H, Pan Y, He Y, Synthesis and characterization of FeCoNiCrCu high-entropy alloy coating by laser cladding, Materials and Design, 32(2011)1910-1915.

Zhong M, Liu W, Laser surface cladding: the state of the art and challenges, Proc. Mechanical, Vol. 224 Part C: J. Mechanical Engineering Science, Proceedings of the Institution of Mechanical Engineers Part C, Journal of Mechanical Engineering Science, 241(2010)1041-2060.